Theoretical Study of the Formation of Three-Electron Bonds in Some F-Substituted Thiol and Sulfide Anions

Christine Dézarnaud-Dandine*,† and Alain Sevin‡

Contribution from the Laboratoire de Chimie Physique-Matière et Rayonnement, URA 176 of the CNRS, Université Pierre et Marie Curie, 11 Rue Pierre et Marie Curie, 75131 Paris Cedex 05, France, and Laboratoire de Chimie Théorique, UPR 9070 of the CNRS, Université Pierre et Marie Curie (Case 137), Tour 22-23, 4 Place Jussieu, 75252 Paris Cedex 05, France

Received July 24, 1995[⊗]

Abstract: The possibility of formation of stable unsymmetrical three-electron (3e) bonds of the type $\{RS\cdot\cdot(-)\cdot\cdot R'\}$ was theoretically studied by ab initio SCF-CI quantum calculations. It was predicted, on the basis of a classical resonance scheme, that a 3e bond was the most likely to be observed when both constituting fragments RS and R′ had the same electron affinity (EA). In this context the $CH_{3-n}F_nSH$ and $CH_{3-n}F_nSCH_{3-n}F_n$ ($n = 0, 3$) molecules were tested. The results support the prediction for the CF_3/SH^- and CF_3/SCH_3^- anions. By comparing results from different types of basis sets, for describing the valence part of the reaction coordinate or providing the system with the possibility of electron attachment (or detachment) via a very diffuse available space, we were able to propose a qualitative model which accounts for the general features of these processes, in each type of molecule. Semiquantitative data are offered for further experimental testing of our findings with molecules such as $CH_nX_{3-n}SH$ and $CH_nX_{3-n}SCH_3$ (X = F, Cl, Br; $n = 0,1$).

Introduction

In the gas phase, aliphatic thiols and sulfides are good electron acceptors, as shown by ETS measurements.[1] However, although temporary states are easily observed upon electron attachment, the formation of stable anionic species resulting from the capture of one electron by the target molecule is only infrequently observed. For the sake of discussion, let us deal with a hypothetical R′SR molecule. In the compact geometry of the neutral ground state (GS), the uptake of one electron generally leads to a vertical endothermic process: $R'SR + e^- \rightarrow \{R'SR\}^-$. This results from the fact that in the vertical electron attachment the incoming electron is captured by a low-energy valence σ^* molecular orbital (MO) of the neutral molecule, say $\sigma^*(S-R)$.[2] The short SR bond, then containing three electrons, lies in the repulsive part of its potential energy surface (PES). It is only via a major bond relaxation that the anion can reach a stationary point in its PES. For example, in H_2S_2, which forms a stable anionic species, experimentally observed,[3a,f] the SS bond length is 2.0824 Å in the GS, while it is 2.8080 Å in the anionic species (values calculated at the MP2/6-311G** level).[3] On the grounds of both experimental and theoretical[4] studies, a set of criteria might be proposed for the formation of stable anions involving three-electron (3e) σ bonds: (i) the neutral molecule must possess low-energy σ^* MOs; (ii) the σ bond which is likely to accommodate a third electron must be composed of electronegative fragments able to retain it from fast detachment; (iii) valence bond (VB) studies of 3e bonds have shown that the energy stabilization of the system essentially comes from the resonance between two limiting localized electronic structures,

$$\{R'S^0\cdots R^-\} \leftrightarrow \{R'S^-\cdots{}^0R\}$$

and that this resonance is maximum when both systems are of equal energy at infinite separation. After the definition of electron affinity EA, that is, $EA(X) = E(X^0) - E(X^-)$, where $E(X)$ stands for potential electronic energy of X, this condition amounts to another simple one: the resonance will be maximum when both fragments have the same EA, or, when the EAs are as close as possible when dealing with nonsymmetrical fragments. Though it is clear that all these requirements are fulfilled in symmetrical molecules such as H_2S_2 and its associated anion $H_2S_2^-$, an important question arises regarding the possible formation of such 3e bonds with nonsymmetrical structures. In a previous theoretical study,[5] we calculated the thermodynamic balance between both ends of the preceding resonance scheme,

† Laboratoire de Chimie Physique-Matière et Rayonnement.

‡ Laboratoire de Chimie Théorique.

⊗ Abstract published in *Advance ACS Abstracts,* April 15, 1996.

(1) (a) Modelli, A.; Distefano, G.; Jones, D. *Chem. Phys.* **1982**, *73*, 395−401. (b) Modelli, A.; Jones, D.; Colonna, F. P.; Distefano, G. *Chem. Phys.* **1983**, *77*, 153−158. (c) Modelli, A.; Distefano, G.; Guerra, M.; Jones, D.; Rossini, S. *Chem. Phys. Lett.* **1986**, *132*, 448−449. (d) Modelli, A.; Jones, D.; Distefano, G.; Tronc, M. *Chem. Phys. Lett.* **1991**, *191*, 361−366. (e) Dézarnaud, C.; Tronc, M.; Hitchcock, A. P. *Chem. Phys.* **1990**, *142*, 455−462. (f) Dézarnaud, C.; Tronc, M.; Modelli, A. *Chem. Phys.* **1991**, *156*, 129−140.

(2) (a) Modelli, A.; Guerra, M.; Jones, D.; Distefano, G.; Irgolic, K. J.; French, K.; Pappalardo, G. C. *Chem. Phys.* **1984**, *88*, 455−461. (b) Guerra, M.; Distefano, G.; Jones, D.; Colonna, F. P.; Modelli, A. *Chem. Phys.* **1984**, *91*, 383−390. (c) Modelli, A.; Distefano, G.; Guerra, M.; Jones, D.; Rossini, S. *Chem. Phys.* **1986**, *125*, 389−390. (d) Modelli, A.; Scagnolari, F.; Distefano, G.; Guerra, M.; Jones, D. *Chem. Phys.* **1990**, *145*, 89. (e) Jordan, K. D.; Burrow, P. D. *Chem. Rev.* **1987**, *87*, 557−588.

(3) Optimized at the MP2/6-311G** level, C. Dézarnaud-Dandine and A. Sevin, unpublished results. Similar values have also been found: (a) Franzi, R.; Geoffroy, M.; Reddy, M. V. V. S.; Weber, J. *J. Phys. Chem.* **1987**, *91*, 3187−3190. (b) Zhu, J.; Petit, K.; Colson, A. O.; DeBolt, S.; Sevilla, M. D. *J. Phys. Chem.* **1991**, *95*, 3676−3681. (c) The same value is also found in the 3e bond of $H_2SSH_2^+$: Knop, O.; Boyd, R. J.; Choi, S. C. *J. Am. Chem. Soc.* **1988**, *110*, 7299−7301. (d) Symons, M. C. R. *J. Chem. Soc., Perkin Trans. 2* **1974**, 1618−1620. (e) Nelson, D. J.; Peterson, R. L.; Symons, M. C. R. *J. Chem. Soc., Perkin Trans. 2* **1977**, 2005−2015. (f) Marignier, J. L.; Belloni, J. *J. Phys. Chem.* **1981**, *85*, 3100−3105.

(4) (a) Pauling, L. *J. Am. Chem. Soc.* **1931**, *53*, 3225−3237. (b) Pauling, L. *J. Chem. Phys.* **1933**, *1*, 56−59. (c) Meot-Ner, M.; Hamlet, P.; Hunter, E. P.; Field, F. H. *J. Am. Chem. Soc.* **1978**, *100*, 5466−5471. (d) Meot-Ner, M. *Acc. Chem. Res.* **1984**, *17*, 186−193. (e) Clark, T. *J. Am. Chem. Soc.* **1988**, *110*, 1672−1678. (f) Baird, N. C. *J. Chem. Educ.* **1977**, *54*, 291−293. (g) Gill, P. M. W.; Radom, L. *J. Am. Chem. Soc.* **1988**, *110*, 4931−4941. (h) Komiha, N.; Daudey, J. P.; Malrieu, J. P. *J. Phys. B: At. Mol. Phys.* **1987**, *20*, 4375−4391. (i) Hiberty, P. C.; Jumbel, S.; Danovich, D.; Shaik, S. *J. Am. Chem. Soc.*, submitted for publication. (j) Hiberty, P. C.; Humbel, S.; Archirel, P. *J. Phys. Chem.* **1994**, *98*, 11697−11704.

(5) Dézarnaud-Dandine, C.; Sevin, A. *Chem. Phys.* **1995**, *197*, 51−59.

S0002-7863(95)02480-2 CCC: $12.00

Table 1[a]

compd	MP2/6-311G**	MP2/6-311++G** [b] and others[c−e]	EA (exptl)
1, CH_3SH	−438.035 016	−438.037 332	−2.85 (refs 1f, 14, 16)
1va	−437.933 747	−438.005 741	
	[−2.75]	[−0.86][b]	
2, CH_3SCH_3	−477.227 528	−477.231 065	−3.25 (refs 1f)
2va	−477.112 659	−477.186 632	
	[−3.12]	[−1.21][b]	
3, CF_3SH	−735.269 661	−735.289 558	
3va	−735.183 121	−735.255 170	
	[−2.35]	[−0.93][b]	
3(3e), $\{CF_3\therefore SH\}$	−735.232 241	−735.262 460	
	[1.02][f]	[0.74][f]	
4, CF_3SCH_3	−774.463 834	−774.484 432	
4va	−774.372 307	−774.455 639	
	[−2.49]	[−0.78][b]	
4(3e) $\{CF_3\therefore SCH_3\}$	−774.417 381	−774.447 708	
	[1.16][f]	[1.00][f]	
5, H	EUHF −0.499 810	EUHF −0.499 818	0.75 (refs 17−19)
5a, H^-	−0.482 913	−0.505 611	
	[−0.44]	[0.16][b]	
		[0.26][c]	
6, SH	−398.204 824	−398.206 103	2.31−2.32 (refs 20−22)
6a, SH^-	−398.270 957	−398.273 510	
	[1.80]	[1.83 (MP4 1.79)][b]	
		[2.19][d]	
7, CH_3 (D_{3h})	−39.707 238	−39.708 661	0.06 (refs 23−25)
7a, CH_3^- (C_{3v})	−39.670 291	−39.696 018	0.08 (refs 19, 26, 27)
	[−1.00]	[−0.34 (MP4 −0.28)][b]	
		[0.10][d]	
8, CF_3 (C_{3v})	−336.942 521	−336.958 267	1.70−1.84 (refs 26, 28−30)
8a, CF_3^- (C_{3v})	−336.969 409	−337.012 297	
	[0.73]	[1.47 (MP4 1.59)][b]	
		[1.52][c]	
9, CH_3S (C_{3v})	−437.397 157	−437.399 402	1.82−1.90 (refs 26, 31, 32)
9a, CH_3S^- (C_{3v})	−437.449 849	−437.453 508	
	[1.13]	[1.47 (MP4 1.43)][b]	
		[1.78][d]	
10, CF_3S (C_{3v})	−734.625 542	−734.646 401	
10a, CF_3S^- (C_{3v})	−734.729 016	−734.759 683	
	[2.81]	[3.08 (MP4 3.02)][b]	
		[3.33][e]	

[a] All energies are in a.u. Between square brackets are given the calculated EAs (eV) obtained at various levels of calculations. The MP2/6-311G** optimized geometries are as follows. **6** SH 1.3381. **6a**: SH 1.3428. **7**: CH 1.0792. **7a**: CH 1.1221, HCH 101.63. **8**: CF 1.3179, FCF 111.32. **8a**: CF 1.4337, FCF 99.53. **9**: CH 1.0921, CS 1.7980, HCS 110.19. **9a**: CH 1.0995, CS 1.8265, HCS 112.34. **10**: CF 1.3366, CS 1.8056, FCS 110.99, FCF 107.91. **10a**: CF 1.3805, CS 1.7334, FCS 115.34, FCF 103.02. [b] MP2/6-311++G**. [c] MP2/6-311++G**(3df,2p). [d] MP4/6-311++G**(3df,2p). [f] Energy difference (eV) between the neutral GS and the optimized 3e structure given in Figure 1.

for a series composed of fragments resulting from the cleavage of saturated F-substituted thiols and sulfides, and found that compounds like CF_3SH (**3**) and CF_3SCH_3 (**4**) are potential candidates for 3e bond formation. We present here a further theoretical investigation of these molecules and their related anions, to which we have added CH_3SH (**1**) and CH_3SCH_3 (**2**) for the sake of comparison. It is noteworthy that our aim is principally to seek the chemical obtention of *stable* 3e species, observable for example in matrices or neutral media, rather than to study the physical aspects (cross sections etc.) of the temporary anion states (shape resonances) that might be formed with the same species, at high energy.

Computational Details

All calculations were performed with the Gaussian 92 series of programs.[6] The RHF Hamiltonian was used for singlet species and the UHF Hamiltonian for doublet species. Four basis sets were used. The first one, 6-311G**,[7] which provides good valence and polarization functions, will be referred to as VP in the coming sections. It was used throughout for full geometry optimization at the MP2 level. This basis set is likely to yield accurate results as long as valence MOs are of concern. In order to take into account the potential need for Rydberg and, more generally, diffuse space, in anionic species, all calculations were repeated on the previously optimized geometries at the MP2/6-311++G**[8] level, referred to as VPD. For describing the fragments, either radicals **5**−**10** or anions **5a**−**10a** (Table 1), the more complete basis sets 6-311++G(3df,2p) or 6-311G(3df,2p)[9] were used for MP4 (SDTQ) calculations. Finally we also used a basis in which the 6-311++G** set was augmented by very diffuse s-type functions on S and C, of exponent 0.0005, still at the MP2 level, and referred to as VPDD in coming discussions (vide infra).[10] In UHF runs, we checked that spin contamination remained negligible and not likely to affect significantly the corresponding calculated geometries and the energies of stationary points. The latter requirement can be easily fulfilled by comparing the calculated MP2 energy (EUMP2) to the projected energy

(6) Frish, M. J.; Trucks, G. W.; Head-Gordon, M.; Gill, P. M. W.; Wong, M. W.; Foresman, J. B.; Johnson, B. G.; Schlegel, H. B.; Robb, M. A.; Reploge, E. S.; Gomperts, R.; Andres, J. L.; Raghavachari, K.; Binkley, J. S.; Gonzalez, C.; Martin, R. L.; Fux, D. J.; De Frees, D. J.; Baker, J.; Steward, J. J. P.; Pople, J. A. *Gaussian 92*, Revision b; Gaussian Inc.: Pittsburgh, PA, 1992.

(7) Francl, M. M.; Pietro, W. J.; Hehre, W. J.; Binkley, J. S.; Gordon, M. S.; De Frees, D. J.; Pople, J. A. *J. Chem. Phys.* **1982**, *77*, 3654−3665 and references cited therein.

(8) Curtiss, L. A.; Jones, C.; Trucks, G. W.; Raghavachari, K. *J. Chem. Phys.* **1990**, *93*, 2537−2545.

(9) Curtiss, L. A.; Nobes, R. H.; Pople, J. A.; Radom, L. *J. Chem. Phys.* **1992**, *97*, 6766−6773.

(10) Glaser, R.; Chog, G. S. C. *J. Phys. Chem.* **1993**, *97*, 3188−3198.

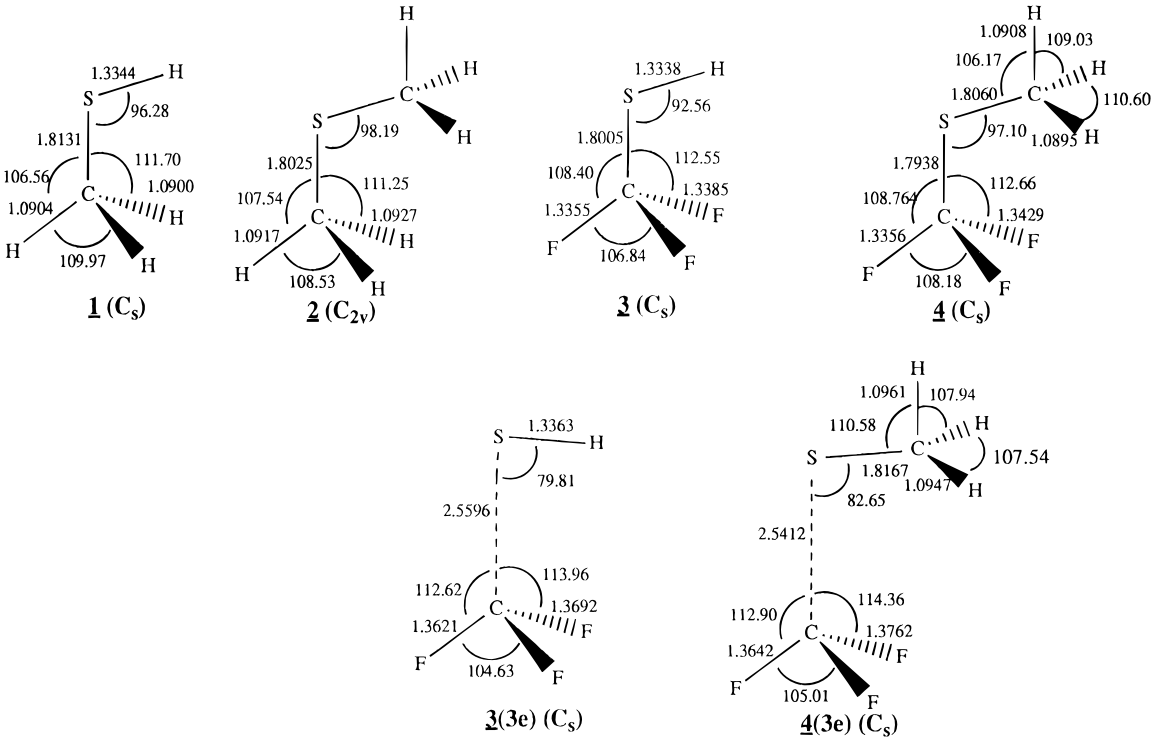

Figure 1. Optimized structures (MP2/6-311G**) of the neutral compounds **1**−**4**. The optimized geometries (MP2/6-311G**) of the anionic species **3**(**3e**) and **4**(**3e**) correspond to the formation of typical CS 3e bonds.

Table 2. Energy Difference (eV) between the Neutral GS and the Fragments at Infinite Separation[a]

parent molecule	products	MP2/6-311G**	MP2/6-311++G**
CH_3SH, **1**	$\{CH_3^0 + SH^0\}_\infty$	3.34	3.33
	$\{CH_3S^0 + H^0\}_\infty$	3.74	3.75
	$\{CH_3^0 + SH^-\}_\infty$	1.55	1.50
	$\{CH_3S^- + H^0\}_\infty$	2.38	2.29
CH_3SCH_3, **2**	$\{CH_3^0 + CH_3S^0\}_\infty$	3.35	3.35
	$\{CH_3^0 + CH_3S^-\}_\infty$	1.92	1.87
CF_3SH, **3**	$\{CF_3^0 + SH^0\}_\infty$	3.33	3.40
	$\{CF_3S^0 + H^0\}_\infty$	3.93	3.90
	$\{CF_3^0 + SH^-\}_\infty$	1.53	1.57
	$\{CF_3S^- + H^0\}_\infty$	1.11	0.82
CF_3SCH_3, **4**	$\{CF_3S^0 + CH_3^0\}_\infty$	3.56	3.52
	$\{CF_3^0 + SCH_3^0\}_\infty$	3.45	3.45
	$\{CF_3^0 + CH_3S^-\}_\infty$	1.94	1.98
	$\{CF_3S^- + CH_3^0\}_\infty$	0.75	0.44

[a] The reference energies are given in Table 1.

(PMP2) which eliminates the eventual spin contamination.[11] The calculated structures and data are given in Figure 1 and Tables 1 and 2.

Discussion of Results

In the first step, we briefly examine the structure and energies of the neutral molecules **1**−**4** and their associated vertical anions, labeled **1va**−**4va** in Table 1. For the anions, the vertical energy has been obtained with the frozen geometry of the neutral GS. In a second step we study the various fragments, either radicals or anions, formed by the cleavage of the SH or SC bonds of the aforementioned compounds. Their geometries have been optimized in each case. In the coming discussion, it is practical to use the calculated EAs for which experimental values are generally available. These quantities have been obtained by taking the electronic potential energy differences, with no further correction. The structures of molecules **1**−**4** are displayed in Figure 1.

Molecules 1−4 and Their Vertical Anions 1va−4va. Upon examination of the GS geometries of **1**−**4**, one sees that F-substitution does not produce important structural changes. Previous ETS and theoretical studies have established that the lowest energy vertical anions of such molecules might be qualitatively described as species with the extra electron located in the lowest energy antibonding valence σ^* MO. The corresponding MO-CI eigenstates generally are made of a complex mixture of valence and Rydberg components sharing strong analogies with low-energy valence lone pair → σ^* excited states involving the same virtual MO.[12] Their actual nature will not be discussed here. In a previous theoretical study, we have shown that the electron acceptor properties of a given thio compound to some extent depend on the actual CS bond length(s): long CS bonds are associated with low-energy σ^* MOs, with a good propensity for accommodating an extra electron at low energy cost.[13] When dealing with molecules **1**−**4**, no important bond length variation is observed and, accordingly, no clear-cut trend is observed in the vertical energies of the lowest energy anion state, calculated by the VP method. The important negative EAs thus obtained result from the fact that the extra electron is constrained to be located in a compact σ^* MO, whose CS distance corresponds to the repulsive region of the anion PES. The resulting metastable situation that results is typical of temporary anion states for which shape resonances are experimentally observed, followed by fast electron detachment. In contrast, the VPD EAs reveal drastic energy changes compared to the preceding ones. With this basis set, the electron is not really linked to the molecule, being located far from the molecule in a diffuse space. If even more room is provided for it, as for example with the VPDD method, the calculated energy of the anionic system drops to that of the neutral GS, clearly showing that the electron is ejected from the molecule

(11) (a) Heinrich, N.; Koch, W.; Frenking, G. *Chem. Phys. Lett.* **1986**, *124*, 20−25. (b) Guerra, M. *Chem. Phys. Lett.* **1990**, *167*, 315−319.

(12) (a) Mouflih, B.; Larrieu, C.; Chaillet, M. *New J. Chem.* **1988**, *12*, 65−69. (b) Sevin, A.; Dézarnaud-Dandine, C.; Tronc, M. *Chem. Phys.* **1992**, *165*, 245−255.

(13) Dézarnaud-Dandine, C.; Sevin, A. *J. Mol. Struct. (THEOCHEM)* **1995**, *339*, 133−142.

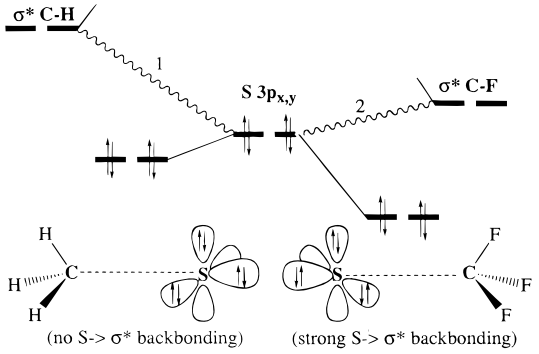

Figure 2. Schematic diagram showing the back-bonding interactions arising between the doubly occupied MOs of the lone pairs borne by S, labeled $3p_{x,y}$ for the sake of simplicity, and the σ^* MOs of either CF_3 (right) or CH_3 (left). It is assumed that the system possesses a C_{3v} local symmetry.

though, in some way, artificially present in the calculation. Thus, we see that the VP method affords a description of the real vertical electron attachment process, while the addition of very diffuse functions yields an efficient electron detachment channel. For example, for CH_3SH (**1**), our calculated VP value of −2.75 eV is in good agreement with ETS measurements (−2.85 eV),[1f] as well as with previous theoretical studies.[14] In coming sections, we will exploit this possibility for describing the adiabatic evolution of the anions over a wide range of the CS bond lengths, the latter being considered as a true reaction coordinate (RC) (vide infra).

Radicals 5−10 and Anions 5a−10a. The basis set dependence is less accentuated when dealing with these fragments. With the exception of CH_3 (**7**, **7a**) calculated at the VP level, they all have positive EAs (Table 1). For all these moieties, the best agreement with experimental values, when available, is provided by MP4/6-311++G(3df,2p) data. The difficulty of obtaining accurate values of the EA for H or CH_3 at our level of calculation is well-known and requires no special comment since, at any rate, this fragment does not play a crucial role in the coming discussion of the PESs. However, the latter point reminds us that our study remains at the semiquantitative level. Some general features emerge from the examination of the structures and energies. When comparing the various radical and anion pairs, one sees that in the anions noticeable bond relaxation occurs, compared with the radical geometry. The biggest variation is found for the CF_3 pair **8** and **8a**, in which the CF bond lengths are respectively 1.3719 and 1.4337 Å, along with a pyramidalization angle substantially increased in **8a**. An interesting fact arises from the behavior of the CS bond in the pairs CH_3S/CH_3S^-, on the one hand, and CF_3S/CF_3S^-, on the other hand. While, for the first couple, the CS bond length increases in the anion (1.8265 Å versus 1.7980 Å), it is the opposite for the second couple, where the CS bond length is longer in the radical (1.8056 Å versus 1.7334 Å). A qualitative argument, schematically drawn in Figure 2, might be proposed: in CF_3S^-, there is a strong back-bonding from the two $3p_{x,y}$ lone pairs of the S atom, into the σ^*_{CF} MOs.[15] Taking CH_3S^- as a reference, in CF_3S^- the stretching of the CF bonds lowers the energy of the σ^*_{CF} MOs, thus yielding a stronger 2e interaction. This effect is enhanced by both CF bond length relaxation and concomitant CS shortening. The phenomenon is no longer observed in CH_3S (**9**, **9a**), for which the σ^*_{CH} MOs remain essentially out of reach. The strong stabilization of the fluorinated anion is largely responsible for the large EA of CF_3S (**10**), which is twice that of **9**.[16]

In Table 2 are given the energies of the various fragments, at infinite separation, that would result from the cleavage of the SH or CS bonds in molecules **1**−**4** and in the related anions. In all cases, the reference energy is that of the neutral GS. Let us first deal with the homolytic ruptures of the neutral molecules. At a first glance, we see that SH bond cleavage is generally more difficult than CS cleavage by about 0.5 eV in both types of calculations, so that, in the rest of the paragraph, we will restrict ourselves to the discussion of the VPD values. All CS bond energies are close to 3.40 eV, and F-substitution has only a small effect. For example, the bond energy is 3.52 eV for the CF_3S/CH_3 bond while it is 3.45 eV for the CF_3/SCH_3 counterpart. On the contrary, important changes are observed when examining the lowest energy fragments resulting from rupture of the same type of bonds in the anions. First of all, in all cases, the asymptotic anionic systems lie below the parent neutral ones by at least 1.5 eV, due to the positive EAs of the fragments. When comparing CF_3SH^- (**3a**) and $CF_3SCH_3^-$ (**4a**), we see that the high EA of CF_3S makes the ruptures of either CF_3S/H in **3a** or CF_3S/CH_3 in **4a** much preferred. The latter point will be taken into account in the formation of 3e bonds, discussed later on.

Candidates for the Formation of 3e Bonds. Let us recall that the energy criterion mentioned in the introductory part for optimal formation of a stable 3e bond is that both fragments have the same EA. Going back to the data of Table 1, we see that, either by calculation or by experiment, three fragments have very close EAs: SH, CF_3, and CH_3S. Excluding the disulfides, we are thus left with two potential candidates for the formation of stable 3e bonds: $\{CF_3\cdots SH\}^-$ starting from **3a** and $\{CF_3\cdots SCH_3\}^-$ starting from **4a**. No such stable bonds are expected either from CH_3SH^- (**1a**) or $CH_3SCH_3^-$ (**2a**) or from rupture of the second CS bond in $CF_3SCH_3^-$ (**4a**), even though the latter yields a more stable asymptotic system $\{CF_3S^-\cdots{}^0CH_3\}_\infty$ than its counterpart $\{CF_3{}^0\cdots SCH_3^-\}_\infty$. We

(14) Chiu, S. W.; Li, W. K.; Tzeng, W. B.; Ng, C. Y. *J. Chem. Phys.* **1992**, *97*, 6557−6568.

(15) Similar arguments are found in the following: (a) Wiberg, K. B.; Rablen, P. R. *J. Am. Chem. Soc.* **1993**, *115*, 614−625. (b) Rodriquez, C. F.; Hopkinson, A. C. *J. Mol. Struct. (THEOCHEM)* **1993**, *280*, 205−209. (c) Reed, A. E.; Schleyer, P. v. R. *J. Am. Chem. Soc.* **1990**, *112*, 1434−1445.

(16) Leroy, G.; Sana, M.; Wilante, C. *J. Mol. Struct. (THEOCHEM)* **1991**, *228*, 37−45.
(17) (a) Peckeris, C. L. *Phys. Rev.* **1958**, *112*, 1649−1658; (b) **1962**, *126*, 1470−1476.
(18) Lykke, K. R.; Murray, K. K.; Lineberger, W. C. *Phys. Rev. A* **1991**, *43*, 6104−6107.
(19) Kalcher, J.; Sax, A. F. *Chem. Rev.* **1994**, *94*, 2291−2318.
(20) Curtiss, L. A.; Raghavachari, K.; Pople, J. A. *J. Chem. Phys.* **1993**, *98*, 1293−1298.
(21) Eyler, J. R.; Atkinson, G. H. *Chem. Phys. Lett.* **1974**, *28*, 217−220.
(22) Steiner, B. *J. Chem. Phys.* **1968**, *49*, 5097−5104.
(23) Rodriguez, C. F.; Sirois, S.; Hopkinson, A. C. *J. Org. Chem.* **1992**, *57*, 4869−4876.
(24) Kraemer, W. P.; Spirko, V.; Malmqvist, R. A.; Roos, B. O. *J. Mol. Spectrosc.* **1991**, *147*, 526−540.
(25) Salzner, U.; Schleyer, P. v. R. *Chem. Phys. Lett.* **1992**, *199*, 267−274.
(26) Lias, S. G.; Bartmess, J. E.; Liebman, J. F.; Levin, R. D.; Mallard, W. G. *J. Phys. Chem. Ref. Data* **1988**, *17*, Suppl. 1 and references cited therein.
(27) Ellison, G. B.; Engelking, P. C.; Lineberger, W. C. *J. Am. Chem. Soc.* **1978**, *100*, 2556−2558.
(28) (a) Gutsev, G. L. *Chem. Phys.* **1992**, *163*, 59−67; (b) *J. Chem. Phys.* **1993**, *98*, 7072−7080.
(29) Illenberger, E. *Chem. Phys. Lett.* **1981**, *80*, 153−158.
(30) Dispert, H.; Lacmann, K. *Int. J. Mass. Spectrom. Ion Processes* **1978**, *28*, 49−67.
(31) Bartmess, J. E.; Scott, J. A.; McIver, R. T. *J. Am. Chem. Soc.* **1979**, *101*, 6047−6056.
(32) (a) Engelking, P. C.; Ellison, G. B.; Lineberger, W. C. *J. Chem. Phys.* **1978**, *69*, 1826−1832. (b) Moran, S.; Ellison, G. B. *J. Phys. Chem.* **1988**, *92*, 1794−1803.

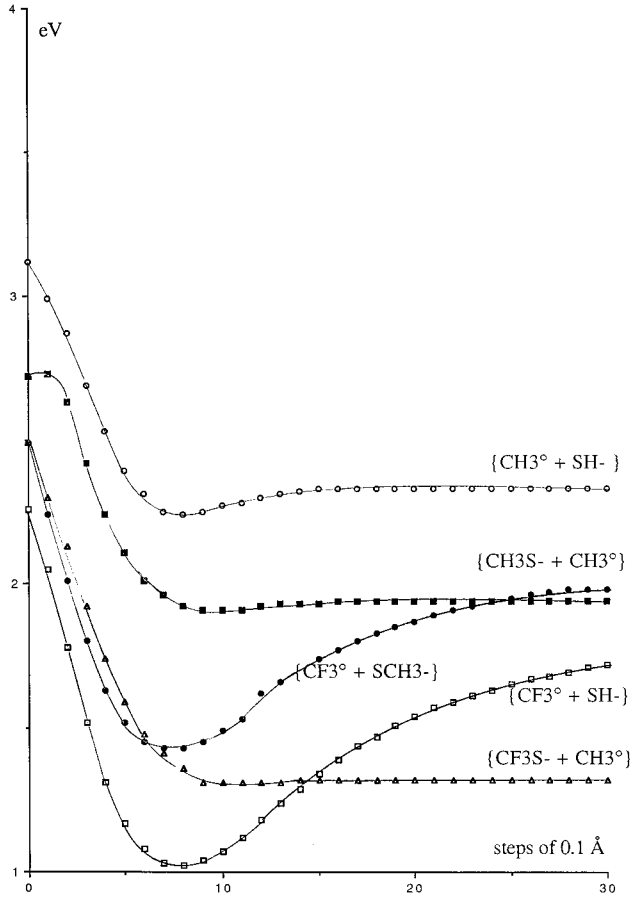

Figure 3. Valence PESs (VP calculations, see text) calculated for the CS elongation of compounds **1a**−**4a**. For each species, the reaction coordinate (abscissa) corresponds to successive increments of 0.1 Å of the CS bond under scrutiny, starting from the GS geometry, displayed in Figure 1, all other geometrical parameters being frozen.

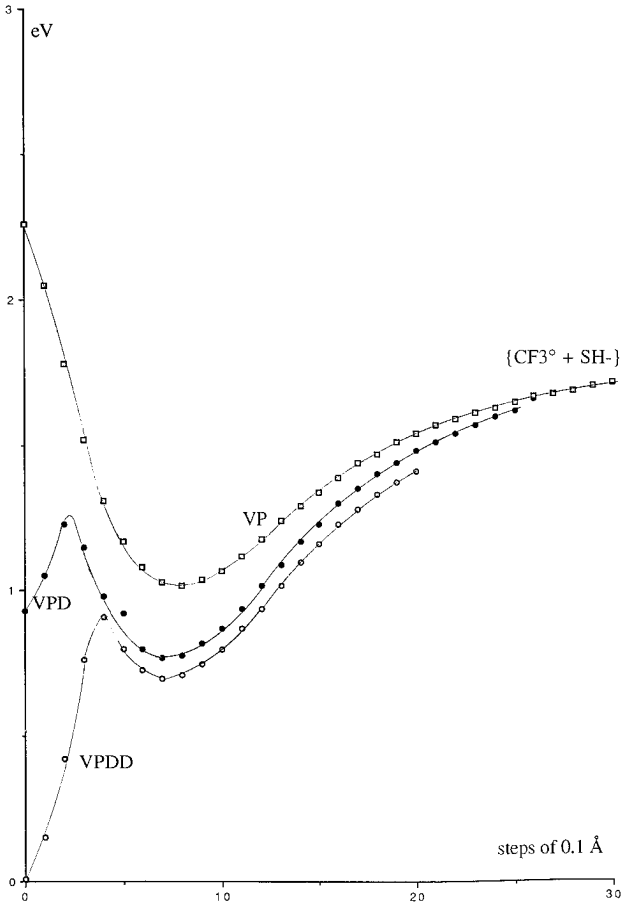

Figure 4. Various types of calculations (VP, VPD, and VPDD) for the CS stretching of CF_3SH^- (**3a**). The reaction coordinate is defined as in Figure 3.

will show in the next section that these predictions are very well supported by the model calculations.

Study of 3e Bond Formation

In order to test our theoretical predictions we qualitatively scanned the various PESs using the following strategy. As the first step, keeping the geometry of the GS frozen, the CS bonds of the anions **1a**−**4a** were stretched by small increments of 0.1 Å, both VP and VPD methods being used. We thus obtained a set of qualitative potential energy profiles. Then, in the second step, the structures of the stationary points were fully optimized at the VP level. Focusing our attention on the valence aspects of the PESs displayed in Figure 3, we see that two typical behaviors are found. The first is observed for the CH_3/SH, CH_3/SCH_3, and CF_3S/CH_3 ruptures. Starting from the GS geometry, as the bond is stretched, the energy decreases and then a plateau is reached, for $R_{CS} \geq 2.5-2.8$ Å. It is noteworthy that the asymptotic energies thus obtained are not equal to the optimal ones given in Table 2 since, during this exploratory scanning, the geometries were not allowed to relax. The second behavior was observed for the CF_3/SH and CF_3/SCH_3 cleavages, which, as expected, exhibit the formation of stable intermediates, for a CS distance which is close to 2.5−2.8 Å. The optimized structures of $\{CF_3\cdots SH\}^-$ (**3**(**3e**)) and $\{CF_3\cdots SCH_3\}^-$ (**4**(**3e**)) are reported in Figure 1 along with their energies.

CF_3SH. Let us now examine the VPD and VPDD results obtained for the CS rupture of **3a**, displayed in Figure 4. For the sake of comparison, the related VP PES already reported in Figure 3 has been added. First of all, it is noteworthy that all three PESs exhibit similar behavior at large distance, and, moreover, show the formation of a stable 3e intermediate in the vicinity of 2.5−2.6 Å (see Figure 1 for actual data). A striking difference is found when either the VP and the VPD or VPDD PESs are compared. Along the VPD PES, at short CS distance, a sharp maximum is found, and then the stable intermediate is reached via a PES which remains roughly parallel to the VP one along the rest of the reaction coordinate. The presence of an energy maximum, at short distance, along the VPD PES is puzzling. The related phenomenon is more clearly understood upon examination of the VPDD PES. We now start from the neutral GS energy; then the energy sharply raises. This part of the PES is nothing but the beginning of the GS dissociation surface, in which the extra electron remains far from the system and plays no role at all. The region of the sharp maximum (around 0.7−0.8 eV) corresponds to the relocalization of this electron on the system, between the separating fragments, leading to the 3e intermediate. Once the potential energy maximum is passed, the VPDD PES remains identical to the VPD one, since the very diffuse atomic orbitals (AOs) no longer have an influence along this part of the coordinate. In reality, we see that these AOs play the crucial role of a reservoir to allow the electron either to remain far from the molecule (to the left of the energy maximum) or to be relocalized in the valence space of the fragments, in an appropriate part of the PES. The shape of the latter PES is better understood with the help of the qualitative analysis displayed in Figure 5.

The classical adiabatic energy profile of the GS PES is shown in broken lines, correlated with $\{CF_3^0\cdots{}^0SH\}_\infty$ on the one hand and, on the other hand, the PES corresponding to the valence behavior of the anion, correlated first with a stable 3e intermedi-

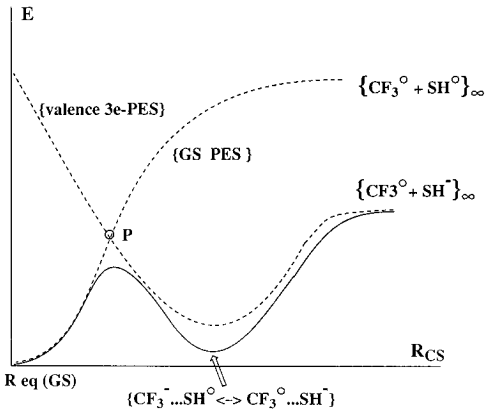

Figure 5. Schematic display of the neutral (GS) and the anionic (valence 3e) PESs (broken lines) leading to the formation of a stable 3e intermediate, as in the case of CF_3SH (see Figure 4). At point P, one gets the contact point between the two types of surfaces, generally yielding a conical intersection when other degrees of freedom are included. The solid-line PES would correspond to an adiabatic situation in which the extra electron is either attached to the molecule (to the right of P) or detached from it (to the left of P).

ate $\{CF_3\cdot\cdot(-)\cdot\cdot SH\}$ and then with $\{CF_3{}^0\cdots{}^-SH\}_\infty$. These two PESs cross at point P. The resulting adiabatic PES, shown in an unbroken line, is therefore constituted of two very distinct parts: starting from the left, before point P, it represents the neutral system with the extra electron not attached to the system. After point P, the behavior is that of the anionic system, previously described. Around point P, the adiabatic maximum depicts the narrow region where the electron is captured by the stretched molecule. In other words, through the artifice of adding ad hoc very diffuse functions, we provide the system with the ability to localize or not localize an extra electron. There exists another way of analyzing Figure 5. In some fashion, the behavior of the broken line PESs recalls that of more or less diabatic surfaces, since, having different numbers of electrons, the representative wavefunctions do not interfere. Therefore, P represents a conical intersection (when other degrees of freedom are taken into account), between both surfaces where a switch from one to the other remains likely, in the direction of either electron attachment (left to right) or electron detachment (right to left). It is more convenient to examine the latter PESs in the following two ways. (i) From right to left, during approach of the anionic fragments we form a stable 3e species that possesses some potential energy excess. If it is released by energy transfer to the surroundings, the 3e intermediate might rest in its lowest energy state and thus have a rather long lifetime. If the energy excess is not efficiently dissipated, the system might reach the energy region of point P where the electron will be detached via a switch toward the GS PES, storing the corresponding energy excess in a hot GS (vibrationally excited). (ii) From left to right, two energy ranges must be examined. If the electron is provided with an energy which places it in the upper part of the valence PES, there is no way for it to be accommodated and it will mostly give rise to short-living resonant states, prior to being detached. If the electron is provided at low energy, around that of P, there is a significant possibility of producing a stable 3e system. In this area, the possibility of tunneling from the GS PES is also likely. If the energy of the incoming electron is progressively raised, we then reach the possibility of dissociating the corresponding anion. All these possibilities are less explicitly described by the adiabatic solid-line PES. The discussion of all other possibilities remains straightforward.[33]

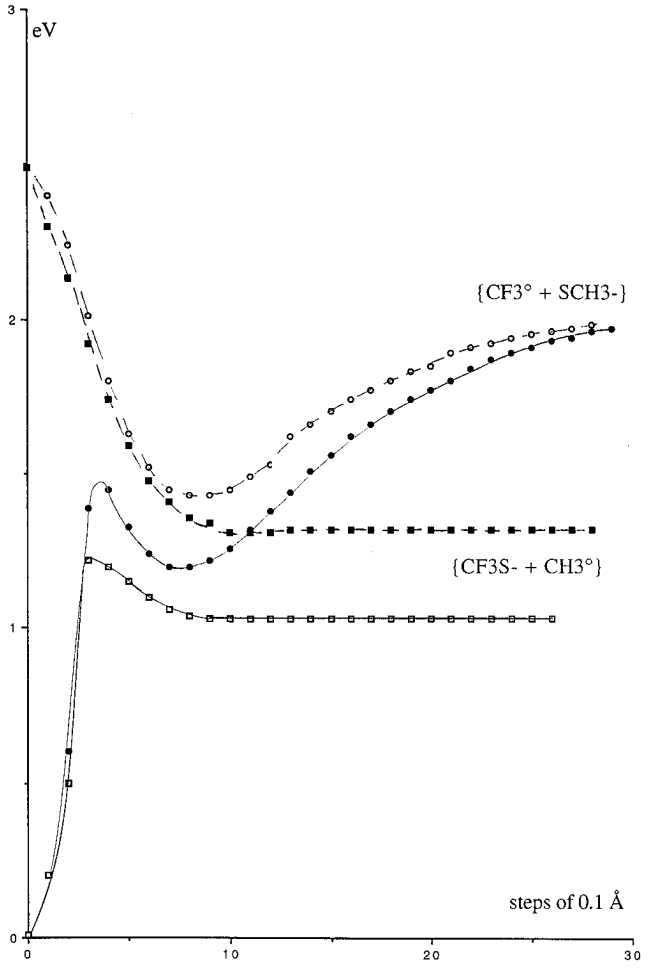

Figure 6. VP and VPDD calculations of the two CS stretchings of CF_3SCH_3 (**4a**), with the same geometrical restrictions as in Figure 3.

CF_3SCH_3. The corresponding PESs are displayed in Figure 6. Two CS ruptures have been reported; the first pair (broken lines) stand for VP PESs and the second (solid lines) for the VPDD PESs. Let us first consider the formation of a 3e bond. As predicted in a preceding section, the CF_3/SCH_3 stretching yields a stable intermediate while the CF_3S/CH_3 cleavage does not. In the latter case, a very weak attraction is nevertheless found at short distance (ca. 2.7 Å) which possibly might result from a weak basis set superposition error (BSSE).[34] In the meantime this shows that the formation of the stable intermediate is not significantly affected by such an effect. When dealing with the VPDD PESs we find in both cases an adiabatic energy maximum at short CS distance, corresponding to the crossing of the valence anionic PES with the GS one (see Figures 4 and 5). Here again, these PESs might be read in two fashions. From right to left, we see that starting from $\{CF_3{}^0\cdots{}^-SCH_3\}_\infty$, the formation of a stable 3e bond through an adiabatic process remains quite unlikely due to the large energy excess stored by

(33) It is worth recalling that the scope of our study is to examine the formation of long-lived stable species and not the formation and evolution of temporary anion states. Accordingly, we have not examined the behavior of the various PESs in terms of real and imaginary parts, within the frame of the Breit−Wigner formula, as developed by J. M. Blatt and V. F. Weisskopf (*Theoretical Nuclear Physics*; J. Wiley & Sons: New York, 1952), or L. D. Landau and E. M. Lifshitz (*Quantum Mechanics*, 2nd ed.; Pergamon Press: London, 1965; Chapter XVIII). A comprehensive discussion and various examples of these aspects are given in the following: Schulz, G. J. *Rev. Mod. Phys.* **1973**, *45*, 379−422, 423−486. On purpose, we remain close to the chemical aspects reviewed by K. D. Jordan and P. D. Burrow (ref 2e) and J. Kalcher and A. F. Sax (ref 19).

(34) Carri, R.; Bonacorsi, R.; Tomasi, J. *Theor. Chim. Acta* **1985**, *68*, 271−283 and references cited therein.

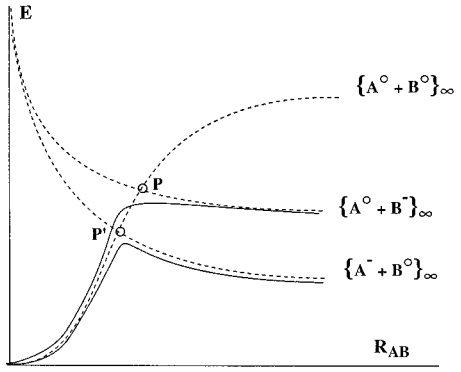

Figure 7. Schematic display of the neutral and the anionic (valence) PESs (broken lines), when no stable 3e intermediate is formed, as in the case of CH_3SH (see Figure 8). At points P and P′, one gets contacts between the two types of surfaces. The solid-line PESs would correspond to adiabatic situations in which the extra electron is either attached to the molecule (to the right of P or P′) or detached from it (to the left of P or P′).

the system which places it above the crossing region and thus leads essentially to electron detachment. Starting from $\{CF_3S^-\cdots{}^0CH_3\}_\infty$, no intermediate can be observed and electron detachment will take place at short CS distance. From left to right, two energy ranges might be considered. At high energy, $\geq$2 eV, only resonant states are likely to be observed. At lower energy, between 1.3 and 1.5 eV, two competitive channels for electron capture exist. The first one, at an energy of 1.3−1.4 eV, leads to the formation of the stable 3e bond, and the second, at slightly lower energy, yields the competitive anionic cleavage of the CF_3S/CH_3 bond. Obviously, this qualitative survey of the reaction coordinate only indicates the various possibilities; they remain to be tested experimentally.

To supplement the schematic information given in Figure 5, Figure 7 might help to explain the PES shape when no 3e bond is formed. In order to take into account the features observed in Figure 6, two cases might be distinguished, according to the relative position of the asymptotic anionic system with respect to the GS energy. When the anionic system is found at low energy, the related PES (solid line) might present an energy maximum, corresponding to the crossing at P′ with the GS PES. No maximum at all is found when the asymptotic anionic system lies at higher energy (crossing at P). This situation is nicely illustrated in Figure 8, where the CS rupture of **1a** is reported. The VP PES shows that, as inferred from resonance consideration, no stable 3e intermediate is formed. The shapes of the VPD and VPDD PESs reveal an abrupt change in the region of 2.3−2.5 Å of the coordinate. It corresponds to the crossing between the GS and the anionic PESs. Starting from the left of the coordinate, we see that there are two possibilities: (i) if the electron is provided to the system with an energy >2 eV, only shape resonance is likely to be observed; (ii) if the electron is provided with an energy between 1.8 and 2 eV, anionic dissociation results. Starting from the anionic system (from right to left), we only observe electron detachment at a CS distance of ≈2.5 Å.

Conclusion

Several features emerge from our analysis of the 3e-bond formation in unsymmetrical compounds. (i) The requirement that both fragments constituting such a bond have the same EA (or EAs as close as possible) is strengthened by the study of CF_3SH^- and even more strikingly illustrated by the different behavior of both CS bonds in $CF_3SCH_3^-$, for which only the CF_3/SCH_3^- rupture yields a stable 3e species. (ii) In quantum

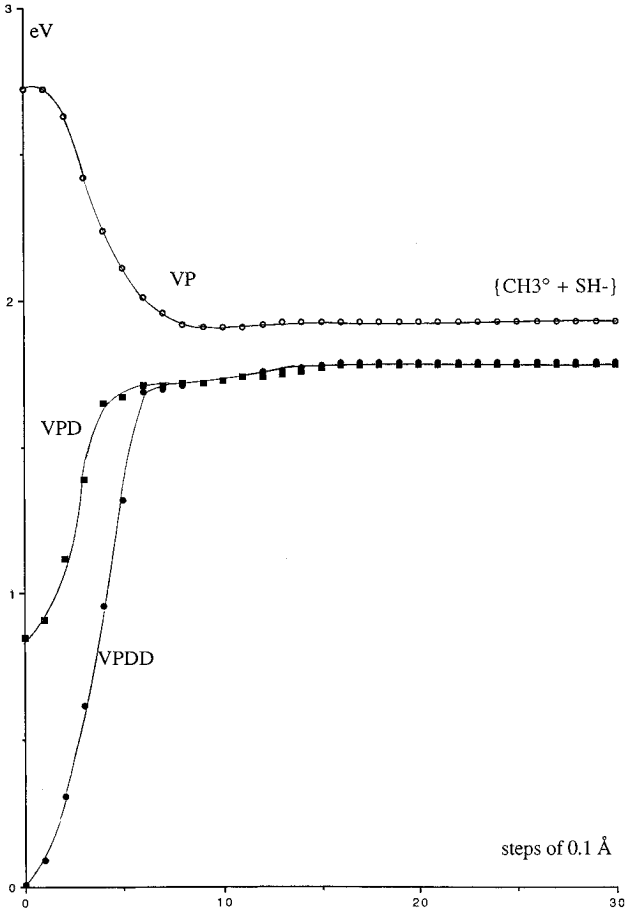

Figure 8. VP, VPD, and VPDD calculations of the CS stretching of CH_3SH (**1a**), with the same geometrical restrictions as in Figure 3.

calculations, the use of basis sets containing diffuse functions, such as VPD, is misleading for a description of the vertical electron attachment process. Alternatively, the use of an even more diffuse basis set, as in VPDD calculations, can show whether or not, in compact structures close to that of the neutral GS, the electron is adiabatically attached to the system. This result can be exploited qualitatively since it provides us with the ability of calculating complete PESs where either neutral or anionic species are observed, depending on the actual region of the CS coordinate. (iii) The crossing between the neutral GS PES and the valence anionic one is crucial for describing the mechanism of electron attachment or detachment. The "memory" of this conical intersection is found along the VPDD PES through the existence of a sharp maximum limiting two very distinct regions of the coordinate. At short CS distance, the most stable system is composed of the neutral molecule plus the extra electron lying distant from it. At long CS distance, the most stable system is composed of either a stable anion having a 3e bond or, more often, of two fragments: a radical plus an anion. It is predicted that electron capture can take place at ca. 0.7−0.8 eV for CF_3SH (Figure 4) and ca. 1.3−1.5 eV (Figure 6) for CF_3SCH_3, leading to stable 3e species. The good agreement of the calculated results with a simple working hypothesis based on consideration of the EAs of the fragments is encouraging and suggests further experimental work in this area. The availability of EAs of various groups such as CCl_3 (2.3 eV), CBr_3 (1.7 eV), and $CHCl_2$ (1.7 eV), though generally known to some approximation,[26] makes thiols and sulfides of general formula $CH_nX_{3-n}H$ and $CH_nX_{3-n}SCH_3$ (X = F, Cl, Br; n = 0,1) potential candidates for this type of study.

JA952480D